ACI STRUCTURAL JOURNAL TECHNICAL PAPER

Title no. 104-S06

Strengthening Concrete Slabs for Punching Shear with Carbon Fiber-Reinforced Polymer Laminates

by Kyriakos Sissakis and Shamim A. Sheikh

This paper describes an innovative approach for strengthening reinforced concrete slabs in shear with carbon fiber-reinforced polymer (CFRP) laminates. A process analogous to stitching is used to retrofit concrete slabs with fiber-reinforced polymer (FRP) strands. The experimental study reported herein was carried out on 28 square, isotropic two-way slab specimens simulating conditions in the vicinity of an interior square column in a continuous flat plate structure. Parameters such as the concrete strength, flexural capacity, and shear reinforcement arrangement were investigated, and the applicability of existing CSA A23.3-04 and ACI 318-05 standard specifications for punching shear resistance were examined. Results from the tests show that marked increases in the punching shear capacity and ductility (over 80 and 700%, respectively) can be achieved with CFRP retrofitting of slabs.

Keywords: flat plate; punching shear; shear reinforcement; slab.

INTRODUCTION

The rehabilitation and strengthening of structural members with composite materials, such as carbon, glass, kevlar, and aramid fiber-reinforced polymers (FRPs), has recently received great attention. Reduced material costs, coupled with labor savings inherent with its lightweight and comparatively simple installation, its high tensile strength, low relaxation, and immunity to corrosion, have made FRP an attractive alternative to traditional retrofitting techniques. Field applications over the last years have shown excellent performance and durability of FRP-retrofitted structures.[1]

Research into the application of externally bonded FRPs to reinforce concrete slabs has concentrated on improving the flexural capacity. There is also the potential for FRP laminates to improve the shear capacity of reinforced concrete slabs. Shear failures occur suddenly and without warning and can be catastrophic, especially in seismic zones. The avoidance of such a failure is of paramount importance; and the benefits from strengthening existing slabs in shear, either for purposes of improved capacity and structural modification or due to deterioration and aging or mistakes in design, are great.

This paper reports on a series of tests conducted to assess the ability of carbon fiber-reinforced polymer (CFRP) laminates to increase the two-way shear capacity of existing reinforced concrete slabs.[2,3] In a pilot test series, three slab specimens retrofitted with CFRP were tested in 2000 and compared with a control specimen.[2] Based on these results, a program was initiated in which 28 square isotropic two-way slab specimens, simply supported on all four sides, were subjected to a concentric monotonically increasing load until failure.[3] Twenty-four of these slab specimens contained CFRP laminate shear reinforcement. The slabs were designed to fail in shear prior to flexure so that the shear strength contribution of the CFRP laminates could be measured. Pilot tests on three slab specimens reinforced in shear found substantial increases in concentric punching shear capacity and ductility.[2] This paper confirms the potential of CFRP laminates to reinforce existing concrete slabs in shear; expands on the influence of variables such as the concrete strength, flexural capacity, and shear reinforcement arrangement on punching shear behavior; and investigates the applicability of existing CSA23.3-04[4] and ACI 318-05[5] standard specifications for punching shear resistance.

RESEARCH SIGNIFICANCE

This research investigates an innovative idea for increasing the two-way shear strength of concrete slabs with FRP. FRP reinforcement is provided in holes that are perpendicular to the plane of the slab in a manner that is equivalent to stitching the slab. The configuration of the holes determines the efficiency of the reinforcement in enhancing the performance of the retrofitted slab. Although the procedure was tested for retrofitting of existing slabs, the results are equally applicable to new structures. With the exception of fire resistance, the procedure proposed herein is considered to be technically superior, easier to implement, and produces more durable structures than traditional strengthening techniques.

THEORETICAL RESPONSE

Concentric punching shear capacity without shear reinforcement

Punching shear failure is characterized by the slab fracturing along planes that extend from the column-slab interface on the compressed face of the slab through the depth of the slab in an inclined direction away from the column. For square columns, the punching shear failure takes the form of a frustum of a pyramid (Fig. 1).

Most research on the shear strength of slabs has been concerned with developing empirical formulas based on a nominal shear stress resistance.[6] Nominal shear stress is obtained by dividing the shearing force by the area of an assumed critical section a certain distance from the column perimeter. The CSA and ACI standards[4,5] assume the shear failure plane to have an angle of inclination of 45 degrees from the slab surface and propose the use of a critical section perimeter half the effective slab thickness from the column periphery (Fig. 2). The depth of the critical section is taken as the effective slab thickness.

In the absence of an unbalanced moment, the shear stress due to factored loads v_f is calculated as

$$v_f = V_f/(b_o d) \tag{1}$$

ACI Structural Journal, V. 104, No. 1, January-February 2007.

MS No. S-2006-035.R1 received February 6, 2006, and reviewed under Institute publication policies. Pertinent discussion including author's closure, if any, will be published in the November-December 2007 *ACI Structural Journal* if the discussion is received by July 1, 2007.

Kyriakos Sissakis *is a Structural Engineer with Halsall Associates Limited, Toronto, Ontario, Canada. His research interests include complex structures, advanced digital applications, and design innovations.*

Shamim A. Sheikh, *FACI, is a Professor of civil engineering at the University of Toronto, Toronto. He is a member of ACI Committee 374, Performance-Based Seismic Design of Concrete Buildings, and a member and former Chair of Joint ACI-ASCE Committee 441, Reinforced Concrete Columns. In 1999, he received the ACI Structural Research Award. His research interests include earthquake resistance of concrete structures, confinement of concrete, use of fiber-reinforced polymer in concrete structures, and expansive cement and its applications.*

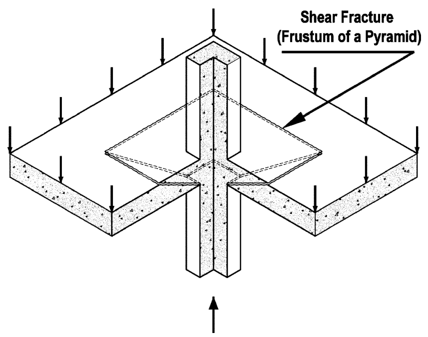

Fig. 1—Punching shear failure.

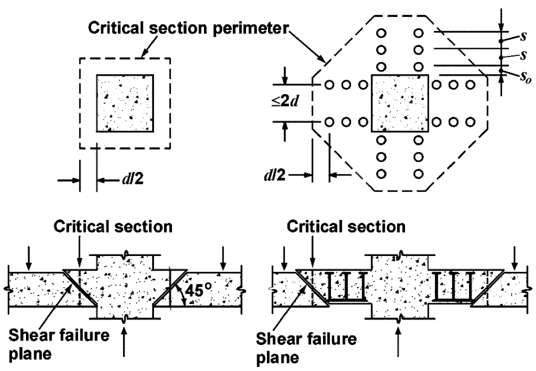

Fig. 2—Critical shear section perimeters for slabs with and without shear reinforcement.

where V_f is the shear force due to factored loads, d is the effective slab thickness for shear, and b_o is the perimeter of the shear critical section $d/2$ from the column periphery. According to the ACI standard,[5] the nominal shear strength for a critical shear section $d/2$ from the column periphery is computed from the smallest of Eq. (2) to (4)

$$v_r = v_c = 0.167\left(1 + \frac{2}{\beta_c}\right)\sqrt{f_c'}\ (\text{MPa}) = \left(2 + \frac{4}{\beta_c}\right)\sqrt{f_c'}\ (\text{psi}) \tag{2}$$

$$v_r = v_c = 0.083\left(\frac{\alpha_s d}{b_o} + 2\right)\sqrt{f_c'}\ (\text{MPa}) = \left(\frac{\alpha_s d}{b_o} + 2\right)\sqrt{f_c'}\ (\text{psi}) \tag{3}$$

$$v_r = v_c = 0.33\sqrt{f_c'}\ (\text{MPa}) = 4\sqrt{f_c'}\ (\text{psi}) \tag{4}$$

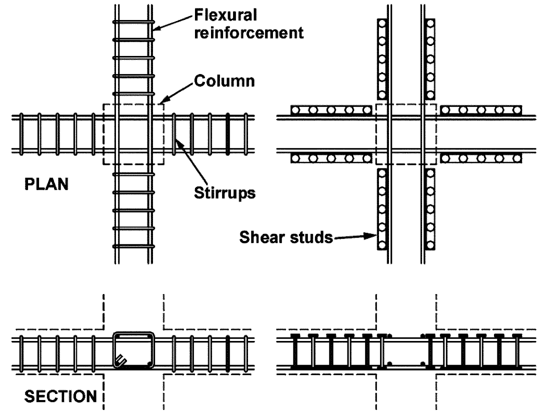

Fig. 3—Closed stirrup and stud shear reinforcement.

where β_c is the ratio of the long to short side of the column, α_s is a modification factor for the support type (α_s = 40 for interior columns), and f_c' is the unconfined concrete compressive strength. The CSA standards'[4] formulation is identical to the aforementioned with the exception of inflated coefficients to compensate for stringent material reduction factors originating from column design.[7] The same applies to Eq. (7) through (11) that follow. Equation (4) governs for the specimens tested in this study. Thus, the concentric load required to fail the slab specimens without shear reinforcement in punching shear[4,5] is

$$P_v = 0.33 b_o d\sqrt{f'_c}(\text{MPa}) = 4 b_o d\sqrt{f'_c}(\text{psi}) \tag{5}$$

Concentric punching shear capacity with shear reinforcement

The CSA and ACI standards[4,5] permit the use of closed stirrups or vertical shear studs as shear reinforcement that are positioned prior to casting and are typically located along perimeters that parallel the column periphery (Fig. 3). Reinforcements of these types also contribute to shear strength by confining the concrete and facilitating the distribution of shearing stresses outwards toward the uncracked concrete. It is proposed that CFRP laminates can be applied to existing slabs within vertical holes drilled through the depth of the slab around the column. The holes can be arranged into a series of perimeters offset from the column in a manner similar to shear stud reinforcement. In new slabs, the FRP reinforcement can be provided in a similar configuration before or after casting.

Concrete slabs reinforced with shear studs can fail in shear outside or within the shear-reinforced zone. Failures can occur within the reinforced zone when the cumulative strength of the shear reinforcement and the concrete is less than the force required to fail the slab in shear outside the reinforced zone or when the shear reinforcement does not sufficiently distribute shearing forces. To ensure adequate distribution of shearing forces, Joint ACI-ASCE Committee 421[8] and CSA Standard[4] specify Eq. (6) through (8) to determine the spacing of shear stud reinforcement.

$$s_o \le 0.40d \tag{6}$$

$$s \le 0.75d \text{ for } v_f \le 0.5\sqrt{f_c'}\ (\text{MPa}) \text{ or } 6\sqrt{f_c'}\ (\text{psi}) \tag{7}$$

$$s \leq 0.50d \text{ for } v_f > 0.5\sqrt{f_c'}\text{ (MPa) or } 6\sqrt{f_c'}\text{ (psi)} \tag{8}$$

In Eq. (6) through (8), s_o is the distance between the column periphery and the first concentric line of shear studs parallel to the column periphery and s is the spacing between consecutive perimeters of shear studs (Fig. 2). In addition, the ACI document[8] recommends that shear studs be positioned at the column corners, in-line with the column face (Fig. 3), and that the spacing of shear studs in the direction parallel to the column face be less than $2d$ (Fig. 2). For this research program, several shear-reinforcing arrangements were investigated. Excessive amounts of shear reinforcement were applied to the slab specimens in an attempt to avoid failures within the shear-reinforced zone. The CSA standard and ACI document,[4,8] however, both impose a limit on the cumulative nominal shear stress resistance of concrete v_c and the shear reinforcement v_s for a critical section $d/2$ from the column periphery to guard against diagonal crushing of the concrete. For headed shear stud reinforcement

$$v_r = v_c + v_s \leq 0.67\sqrt{f_c'}\text{ (MPa) or } 8\sqrt{f_c'}\text{ (psi)} \tag{9}$$

The shear strength of concrete at a critical section varies with distance from the column. The confinement induced by the triaxial stress condition in the vicinity of the column decreases with increasing distance from the column, causing a loss in shear strength. In general, immediately adjacent to the column, a triaxial compressive state exists and at some greater distance the triaxial compressive state dissipates to a uniaxial compressive state. The CSA and ACI standards[4,5] specify a nominal shear strength at a distance $d/2$ from the outermost perimeter of shear reinforcement

$$v_r = v_c = 0.167\sqrt{f_c'}\text{ (MPa)} = 2\sqrt{f_c'}\text{ (psi)} \tag{10}$$

Assuming adequate confinement by the shear-reinforcement, the ultimate concentric load required to fail the slab specimens in punching shear is thus

$$\begin{aligned} P_v &= 0.167bd\sqrt{f_c'} \leq 0.67b_o d\sqrt{f_c'}\text{ (MPa)} \\ &= 2bd\sqrt{f_c'} \leq 8b_o d\sqrt{f_c'}\text{ (psi)} \end{aligned} \tag{11}$$

where b is the perimeter of the critical section $d/2$ from the outermost perimeter of shear reinforcement (Fig. 2 and 4).

Flexural capacity

The flexural capacity of square isotropic two-way slab, simply supported on all four sides and subjected to a concentric square load, can be estimated using Johansen's yield line theory,[9]

$$P_Y = m_r\left[\left(\frac{8}{L/c-1}\right) + 2\pi\right] \tag{12}$$

where L is the length of the supported slab, c is the loading plate side length, and m_r is the flexural capacity of the slab per unit width given by

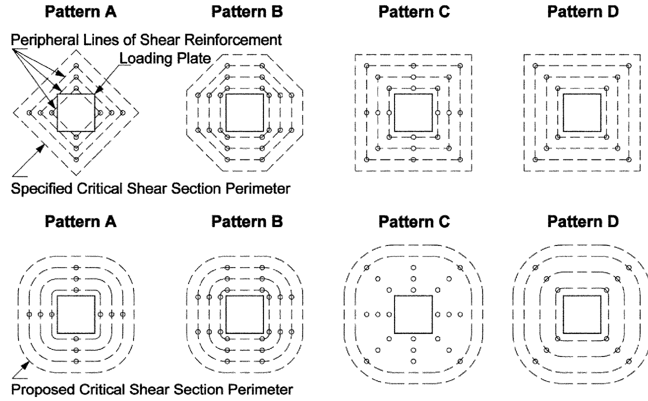

Fig. 4—Shear reinforcement arrangements and assumed critical shear section perimeters of tested slab specimens with three peripheral lines of shear reinforcement.

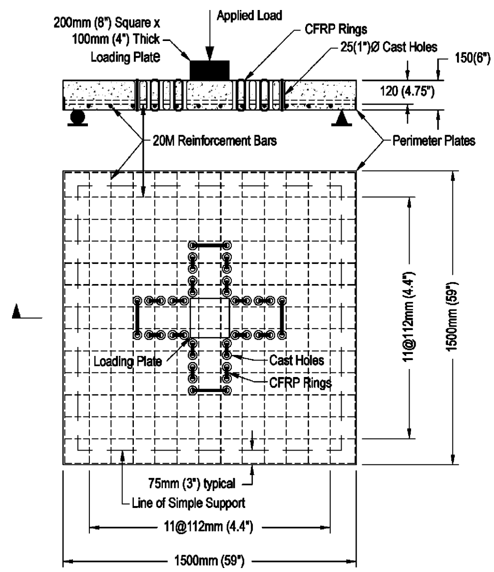

Fig. 5—Slab specimen B5 specifications, load, and supports.

$$m_r = \rho d^2 f_y\left(1 - 0.59\rho\frac{f_y}{f'_c}\right) \tag{13}$$

where ρ, d, and f_y are the flexural reinforcement ratio, depth, and yield strength, respectively. Equation (12) corresponds to a collapse mechanism where the slab yields and divides into quartered circular fans radiating from the corners of a square column. For the specimens in this study, L and c are 1.35 m (53 in.) and 200 mm (8 in.), respectively (Fig. 5).

EXPERIMENTAL PROGRAM

Test specimens

All of the slab specimens had the same external dimensions and contained either 15 M (0.31 in.^{2} area) or 20 M (0.465 in.^{2} area) flexural reinforcement bars. The effective depth was 120 mm (4.75 in.) in both types of flexural reinforcement (Fig. 5). The slabs were cast with normal density concrete in four separate batches, resulting in four different concrete strengths. Each batch consisted of several slab specimens cast with one of the four patterns of 25 mm (1 in.) diameter holes shown in Fig. 4. The holes were later used to reinforce the slabs with CFRP laminates. One slab in each batch was the control specimen and not reinforced in shear.

Table 1—Slab specimen variables and material properties

	Concrete	Flexural reinforcement			Shear reinforcement			Calculated properties	
Specimen	f_c', MPa (ksi)	f_Y, MPa (ksi)	f_U, MPa (ksi)	ρ, %	b, mm (in.)	s/d	A_{CFRP}, mm (in.)/perimeter	P_Y, kN	P_V, kN
Control 1	42.6 (6.18)	428 (62.1)	730 (105.9)	1.49	1280 (50.4)	—	—	643 (144.7)	331 (74.5)
A_4'	42.6 (6.18)	428 (62.1)	730 (105.9)	1.49	2234 (88.0)	0.50	814 (32.0)	643 (144.7)	304 (65.7)
Control 2	36.1 (5.23)	428 (62.1)	730 (105.9)	1.49	1280 (50.4)	—	—	631 (142.0)	305 (68.6)
A_3'	36.1 (5.23)	428 (62.1)	730 (105.9)	1.49	2234 (88.0)	0.75	506/1012/506	631 (142.0)	269 (60.5)
							(19.9/39.8/19.9)		
B_3'	36.1 (5.23)	428 (62.1)	730 (105.9)	1.49	2356 (92.8)	0.75	748 (29.4)	631 (142.0)	284 (53.8)
B_4'					2356 (92.8)	0.50	748 (29.4)		284 (53.8)
C_3'					2960 (116.5)	0.75	924 (36.4)		356 (80.2)
C_4'					2960 (116.5)	0.50	924 (36.4)		356 (80.2)
D_3'					2960 (116.5)	0.75	924 (36.4)		356 (80.2)
D_4'					2960 (116.5)	0.50	924 (36.4)		356 (80.2)
Control 3	34.5 (5.00)	480 (69.6)	623 (90.3)	2.23	1280 (50.4)	—	—	966 (217.4)	298 (67.1)
A_3	34.5 (5.00)	480 (69.6)	623 (90.3)	2.23	1894 (74.6)	0.50	462/924/462	966 (217.4)	223 (50.2)
							(18.2/36.4/18.2)		
A_5	34.5 (5.00)	480 (69.6)	623 (90.3)	2.23	2573 (101.3)	0.50	858/858/660/1320/660	966 (217.4)	303 (68.1)
							(33.8/33.8/26/52/26)		
B_3	34.5 (5.00)	480 (69.6)	623 (90.3)	2.23	2017 (79.4)	0.50	616 (24.3)	966 (217.4)	237 (53.4)
B_5					2697 (106.1)	0.50	792 (31.2)		317 (71.4)
C_3					2480 (97.6)	0.50	792 (31.2)		292 (65.7)
C_5					3440 (135.4)	0.50	1188 (46.8)		405 (91.1)
D_3					2480 (97.6)	0.50	792 (31.2)		292 (65.7)
D_5					3440 (135.4)	0.50	792 (31.2)		405 (91.1)
Control 4	26.6 (3.86)	480 (69.6)	623 (90.3)	2.23	1280 (50.4)	—	—	902 (203.0)	261 (58.7)
A_4	26.6 (3.86)	480 (69.6)	623 (90.3)	2.23	2234 (88.0)	0.50	638 (25.1)	902 (203.0)	231 (52.0)
A_6					2912 (114.6)	0.50	924 (36.4)		301 (67.7)
B_4					2356 (92.8)	0.50	660 (26.0)		244 (54.8)
B_6					3035 (119.5)	0.50	924 (36.4)		314 (70.6)
C_4					2960 (116.5)	0.50	924 (36.4)		306 (68.8)
C_6					3920 (154.3)	0.50	1276 (50.2)		405 (91.2)
D_4					2960 (116.5)	0.50	858 (33.8)		306 (68.8)
D_6					3920 (154.3)	0.50	1254 (49.4)		405 (91.2)

The flexural reinforcement was spaced equally in all the specimens and did not interfere with the holes intended for the CFRP laminates. The development of the flexural reinforcement was attained mechanically by welding the ends of the reinforcing bars to flat steel plates, which occupied the perimeter of the slab specimens (Fig. 5). The number of peripheral lines of shear reinforcement varied between three and six among the slab specimens and the spacing between the consecutive lines was $0.5d$ or $0.75d$. The first perimeter was offset $0.25d$ from the loading plate periphery for all the slab specimens.

Table 1 summarizes the slab specimen details and material properties. The slab specimens with primed pattern labels contained 15 M flexural reinforcement bars, while other slab specimens contained 20 M bars. Those specimens with shear reinforcement are labelled in accordance with their shear reinforcement pattern, A, B, C, or D, with numerical subscripts denoting the number of peripheral lines of shear reinforcement. The amounts of CFRP laminate A_{CFRP} used in each concentric shear-reinforcing perimeter are presented in width of CFRP laminate. For slab specimens A_3', A_3, and A_5, the amount of CFRP laminate applied in each reinforced perimeter varied and is listed in Table 1 starting from the perimeter nearest the loading plate. P_Y and P_V represent the predicted applied loads required to fail the slab specimens in flexural yield and shear, respectively. P_Y is derived from Eq. (12) and P_V is derived from Eq. (5) or (11). The critical shear sections perimeters outside the shear-reinforced zone b, specified by the CSA and ACI standards,[4,5] are depicted in the upper portion of Fig. 4.

A commercially available CFRP system was used. The ultimate tensile strength and tensile modulus per unit width of CFRP laminate was determined experimentally to be 97 kN/m (66.6 kips/ft) and 79.5 MN/m (5452 kips/ft), respectively. The rupture strain was 1.30% and the specified thickness of the CFRP laminate was 0.89 mm (0.035 in.). The CFRP was applied to the slab specimens by cutting long thin strands that could pass through the holes positioned in the slab. The CFRP strands were soaked in epoxy and looped continuously between pairs of holes several times, in a stitch-like manner, until the desired amount of CFRP laminate spanned the depth of the slab (Fig. 5 and 6). The continuous loop of CFRP laminate formed a solid ring of reinforcement that also confined the concrete. Shear reinforcement Pattern A with odd numbers of peripheral lines of shear reinforcement had the two adjacent outer rings of CFRP share a cast hole and as such, the shared hole had twice the CFRP reinforcement (Table 1). The voids that remained after the application of the CFRP laminates were subsequently filled with epoxy.

Specimens in the pilot test series[1] had shorter strands of CFRP laminate that were passed through the cast holes once and had their ends adhered to the top and bottom surfaces of the slab. Large sheets of CFRP laminate were later installed on the top and bottom surfaces to ensure anchorage to the concrete (Fig. 7). The experiment found partial separation of the CFRP laminates from the concrete surface during testing and considerable increases in flexural stiffness and strength due to the added CFRP laminates on the top and bottom surfaces of the specimens. The newly proposed solid rings of CFRP reinforcement minimized the dependence on bond between the concrete and the FRP and avoided increases in flexural strength and stiffness.

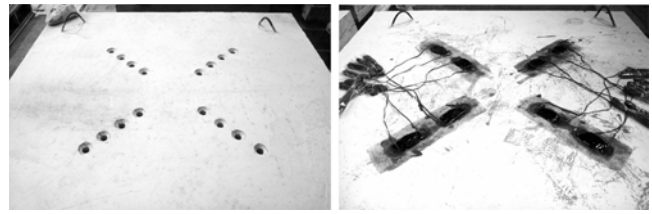

Fig. 6—Slab specimen D4 before and after CFRP application.

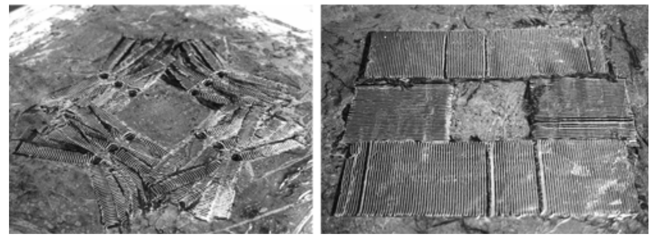

Fig. 7—CFRP application of slab specimen in pilot studies.

Fig. 8—Test setup.

Test setup

The slabs were tested under a vertical monotonically increasing concentric load distributed by means of a 200 mm (8 in.) square by 100 mm (4 in.) thick loading plate. A closed-loop servo-controlled stiff frame test machine (Fig. 8) was used to apply the load in displacement control mode at a rate of 0.01 mm/second (4×10^{-4} in./second). A universal ball joint was attached to the loading plate to prevent moments from being imposed onto the slab specimens.

The slabs were positioned horizontally and simply supported on all four sides by rollers comprised of solid 44 mm (1.75 in.) diameter steel rods. The rollers rested on a steel podium placed directly onto the solid metal base of the test machine. Two of the rollers were welded to the podium, while the opposite two rollers were left free to rotate. The rollers were positioned 75 mm (3 in.) within the edges of the slab specimens. Metal plates 150 x 25 mm (6 x 1 in.) in section, were loosely positioned in between the slab specimens and rollers to distribute bearing forces.

To monitor the displacement of the slab specimens, six linearly variable differential transducers (LVDTs) were used—four to measure the displacements of the supporting structure and two for the displacement of the loading plate. The four LVDTs used to measure the displacement of the supporting structure were positioned at the four corners of the slab, directly above the supporting rollers (Fig. 8).

Local strains in the CFRP laminates and the flexural reinforcement were measured with electrical resistance strain gauges. Four strain gauges were applied with cyanoacrylate adhesive to the lower two central reinforcing bars that passed underneath the loading plate. Two of the gauges were positioned at the middle of the reinforcing bars and the other two were offset 200 mm (8 in.) from the middle in opposing directions. Long-gauge strain gauges were applied to every vertical stem of the CFRP laminate rings. The gauges were adhered to epoxied segments on separate CFRP strands (Fig. 9) that were later attached with epoxy to the solid rings of CFRP reinforcement (Fig. 6). Two gauges were adhered to each strand. The gauges were positioned such that when the strands were applied to the CFRP rings; the gauges were aligned with the center of the slab depth in two adjacent holes. The epoxied segments were formed by sandwiching a small amount of epoxy resin on the CFRP strands between sheets of polyethylene. This made a smooth surface on to which the gauges could be adhered. Several layers of polyurethane and foam mounting tape were applied to all the gauges to prevent moisture penetration and any tangential pressures from being exerted on to the gauges.

EXPERIMENTAL RESULTS

The slabs were designed such that they would fail in shear. With retrofitting, the shear capacity increased significantly causing yield of flexural steel in some slabs. Stress in steel, however, was significantly lower than rupture. Therefore, each slab failed in shear as clearly demonstrated by the failure modes observed during the tests. The results from the tests on the slab specimens are presented in the following. After the description of the failure patterns, responses of the slab specimens are discussed to evaluate different CFRP reinforcement patterns. Theoretical prediction of capacity and the design aspects conclude this section of the paper.

Failure plane description

Figure 10 shows sketches of the shear fractures, portrayed as dotted lines, on the compressed surface of failed slab specimens. Figure 11 shows photographs of the cross sections of selected slab specimens cut in half. The slab specimens were cut such that those with CFRP laminate Patterns A and C had the cut pass through the CFRP laminates and in specimens with reinforcement Patterns B and D the cut passed between the CFRP laminates. The fractures have been

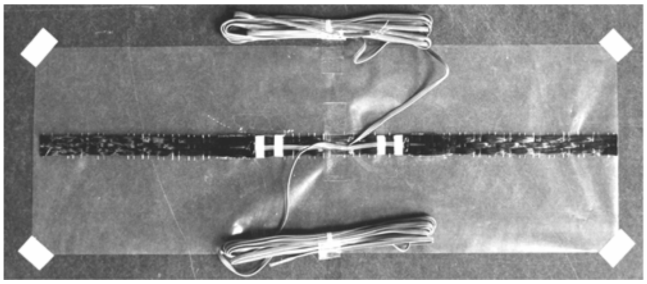

Fig. 9—CFRP strands with adhered strain gauges.

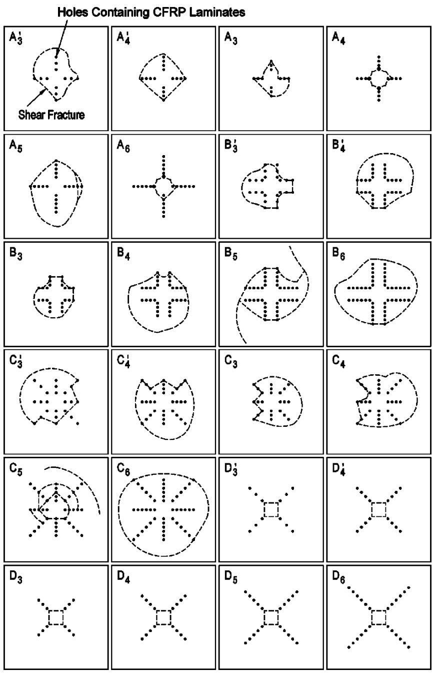

Fig. 10—Sketched slab specimen compressed surface fractures relative shear reinforcement.

highlighted with a black marker. No specimen experienced tensile or compressive flexural failure before failing in shear.

The punching shear failures occurred outside, within or prior to the shear-reinforced zones. In plan, the shear fractures outside the shear-reinforced zone were typically circular in shape. CFRP laminate Pattern A exhibited greater tendency towards shear failures within the shear-reinforced zone than CFRP laminate Patterns B and C. All and only the slab specimens with CFRP laminate Pattern D failed in shear at the perimeter of the loading plate. The specimens with larger spacing of consecutive shear-reinforcing perimeters s were more prone to shear failures within the shear-reinforced zone than the specimens with smaller spacing and equivalent potential critical section perimeters (that is, A_3' versus A_4', B_3' versus B_4', C_3' versus C_4', and D_3' versus D_4').

In section, the shear fractures extended through the depth of the slabs at an angle of inclination generally smaller than 45 degrees. Upon reaching the flexural reinforcement, the failure planes continued horizontally toward the perimeter of the slab between the layers of flexural reinforcement.

Varying degrees of shear and flexural cracking were evident among the slab specimens. The specimens with greater number of shear-reinforcing perimeters, larger consecutive spacing of shear-reinforcing perimeters and lower flexural reinforcement ratios exhibited greater degrees

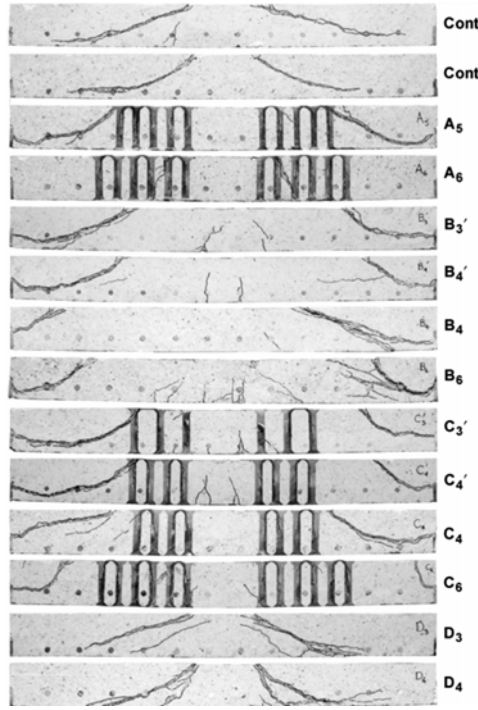

Fig. 11—Photographs of selected slab specimen cross sections.

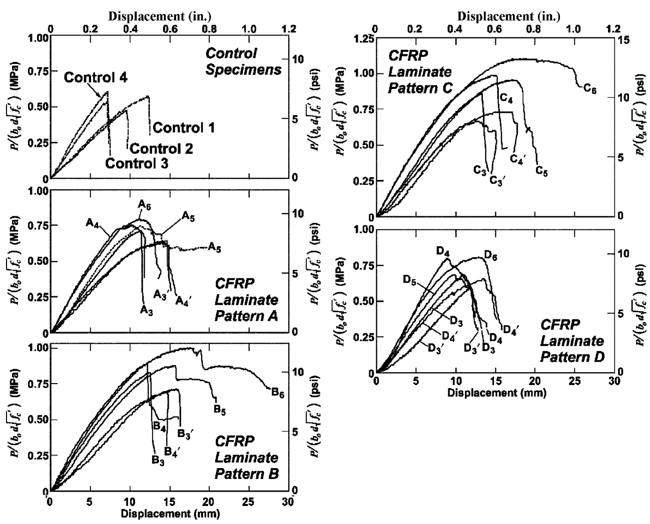

Fig. 12—Slab specimen load-deformation curves.

of concrete cracking within the shear-reinforced zone. For the specimens cut through the CFRP laminates, it was observed that none of the laminates spanned shear fractures, thus implying the specimens did not undergo progressive shear failures within the shear-reinforced zone and that the shear reinforcement and the concrete behaved cohesively.

Load-deformation response

Load-deformation curves for all the tested slab specimens are given in Fig. 12. The slab deformation is taken as the difference between the deflection at the loading plate and the average deflection at the supports. The load has been normalized with respect to $b_o d \sqrt{f'_c}$ to compare specimens with different concrete strengths and corresponds to the cumulative shear stress at a distance of $d/2$ from the loading plate periphery. Table 2 shows the results from all the tests.

The strain energy absorbed U_{80} is taken as the area under the load-deformation curve up to 80% of the ultimate load P_{TEST} beyond the peak. Figure 13 compares the load deformation curves for slab Specimens A_6, B_6, C_6, and D_6, and their respective control specimen. The load-displacement curve for Specimen B_5 is shown in Fig. 14 along with the load-average strain curves for each peripheral line of shear reinforcement and the flexural reinforcement. The CFRP strains and flexural reinforcement strains remained less than 3000με and 6500με, respectively, for all the specimens.

The slab specimens with shear reinforcement demonstrated increases in load carrying capacity and ductility of up to 82 and 768%, respectively, over that of their respective control specimens and, in some cases, changed the mode of failure from punching shear to flexural (refer to $P_{test}/P_{control}$, $U_{80}/(U_{80})_{control}$ and P_{test}/P_Y in Table 2). The increase in shear strength and ductility was accompanied by an increase in audible signs of distress. The formation of a complete shear failure plane was often not instantaneous and formed partially at various sections of the slab, expanding until failure. This growth of the shear failure plane is identified by the slab specimens without abrupt losses of load and/or losses of load followed by plateaus (Fig. 12). As expected, stiffness of the slab specimens with a larger amount of flexural steel was higher than that of specimens with a lower amount of flexural steel. The slab specimens reinforced in shear showed no significant change in stiffness over that of their respective control specimen (Fig. 13).

It can be observed from Fig. 12 and Table 2 that the load-carrying capacity of the slab specimens increased with the increase in the number of CFRP perimeters. The slab specimens with shear-reinforcing Patterns A and D exhibited shear capacity improvements that were approximately half as much as those with shear-reinforcing Patterns B and C. The specimens with larger shear-reinforcing perimeter spacing *s* exhibited no appreciable loss in strength or ductility when compared with the specimens with smaller shear-reinforcing perimeter spacing and equivalent potential critical section perimeters (A_3', and versus A_4', B_3' versus B_4', C_3' versus C_4', and D_3' versus D_4'). *Another important observation that can be made from Fig.* 12 is related to the lack of significant enhancement in deformability and ductility despite the additional CFRP reinforcement in slab specimens of Patterns A and D. Contrary to this behavior, for specimens of shear-reinforcing Patterns B and C in which CFRP is distributed more uniformly, an increase in the number of reinforcement perimeters results in a substantial increase in ductility and hence the energy dissipation capacity of the slabs. Greater increases in ductility, capacity, and audible distress were exhibited with greater numbers of shear-reinforcing perimeters and a greater number of vertical elements of reinforcement in each perimeter.

Failure characteristics

The concrete contribution to shear resistance v_c within the CFRP laminate reinforced zone can be approximated by subtracting the nominal shear resistance of the CFRP laminate shear reinforcement v_{CFRP} from the total shear resistance v_r.

$$v_c = v_r - v_{CFRP} \tag{14}$$

$$v_r = P/bd \tag{15}$$

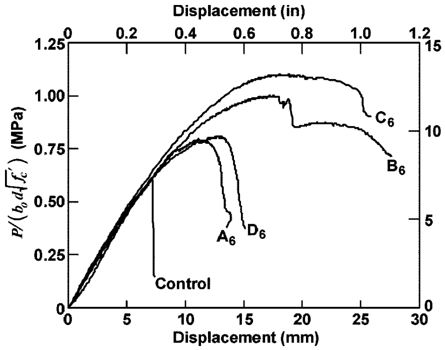

Fig. 13—Load-deformation curves for slab specimens A_6, B_6, C_6, D_6, and Control 4.

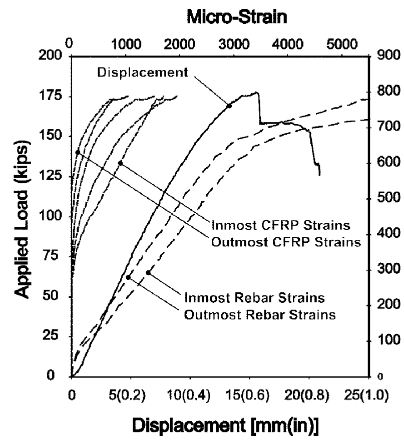

Fig. 14—Load-deformation and stress curves for slab Specimen B_5.

$$v_{CFRP} = (F_{CFRP}\cot\theta)/bs \tag{16}$$

where *P* is the instantaneous applied load, F_{CFRP} is the total tensile force in the CFRP laminates in-line with the assumed shear critical section, *b* is the perimeter of the assumed critical shear section, θ is the angle of inclination of the principle compressive stresses from the slab surface, and *s* is the spacing of the shear-reinforcing perimeters perpendicular from the loading plate periphery. Figure 15 presents the responses of all shear-reinforced perimeters of slab Specimens A_6, B_6, C_6, and D_6 with respect to the applied load. The concrete shear strength was derived from Eq. (14) through (16). Based on the observed angles of inclination of the shear failure planes, a mean angle of 31 degrees was used for θ. The CFRP laminate tensile force was derived from direct strain measurements during testing, such as shown in Fig. 14, the A_{CFRP} given in Table 1, and the experimentally determined CFRP laminate modulus.

Two general observations can be made. First, the concrete shear strength varies with the distance from the loading plate periphery. Perimeters near the plate exhibit higher concrete shear strengths than perimeters further away from the plate. Second, the shearing stresses are distributed differently among the slab specimens. Slab Specimen A_6 shows a gradual increase in shear resistance for all the shear-reinforced perimeters and a sudden loss in shear strength at failure. Slab Specimens B_6 and C_6 also show a gradual increase in shear resistance for all the reinforced perimeters. These specimens, however, portray a gradual loss in shear strength prior to failure. Slab Specimen D_6 shows a gradual loss in shear

Table 2—Slab specimen test results and ultimate analysis

Specimen	Test results		Ultimate analysis									Failure within shear reinforcement (Y/N)
	U_{80}, kJ (ft-kip)	P_{TEST}, kN (kip)	$\frac{P_{TEST}}{b_o d\sqrt{f'_c}}$, MPa (ksi)	$\frac{P_{TEST}}{bd\sqrt{f'_c}}$, MPa (ksi)	$\frac{P_{TEST}}{b_o d\sqrt{f'_c}/\varphi_o}$, MPa (ksi)	$\frac{P_{TEST}}{bd\sqrt{f'_c}/\varphi_o}$, MPa (ksi)	$\frac{P_{TEST}}{P_Y}$	$\frac{P_{TEST}}{P_V}$	$\frac{P_{TEST}}{P_V'}$	$\frac{U_{80}}{(U_{80})_{cont}}$	$\frac{P_{TEST}}{P_{cont}}$	
Control 1	4.0 (2.9)	575 (129)	0.57 (6.9)	0.57 (6.9)	0.41 (4.9)	0.41 (4.9)	0.90	1.74	1.25	—	—	—
Control 2	2.1 (1.5)	439 (99)	0.48 (5.7)	0.48 (5.7)	0.33 (4.0)	0.33 (4.0)	0.70	1.44	1.00	—	—	—
Control 3	1.8 (1.3)	476 (107)	0.53 (6.3)	0.53 (6.3)	0.31 (3.5)	0.31 (3.5)	0.49	1.60	0.89	—	—	—
Control 4	1.9 (1.4)	479 (108)	0.60 (7.3)	0.60 (7.3)	0.34 (3.9)	0.34 (3.9)	0.53	1.83	0.99	—	—	—
Average			—	0.55 (6.5)	—	0.35 (4.1)	—	1.65	1.03	—	—	—
Standard deviation			—	0.06 (0.7)	—	0.04 (0.6)	—	0.17	0.15	—	—	—
A_3'	5.3 (3.9)	591 (133)	0.64 (7.7)	0.37 (4.4)	0.44 (5.3)	0.25 (3.1)	0.94	2.20	1.37	2.52	1.35	N
A_4'	5.9 (4.4)	632 (142)	0.63 (7.6)	0.36 (4.3)	0.45 (5.4)	0.26 (3.1)	0.99	2.16	1.39	1.48	1.10	N
A_3	4.0 (2.9)	646 (145)	0.72 (8.6)	0.48 (5.8)	0.42 (4.8)	0.27 (3.2)	0.67	2.90	1.44	2.22	1.36	Y
A_4	4.6 (3.4)	595 (134)	0.75 (9.0)	0.43 (5.2)	0.42 (4.9)	0.23 (2.8)	0.66	2.58	1.24	2.42	1.24	Y
A_5	6.4 (4.7)	671 (151)	0.74 (8.9)	0.37 (4.4)	0.43 (5.0)	0.21 (2.5)	0.69	2.22	1.10	3.56	1.41	N
A_6	5.3 (3.9)	631 (142)	0.80 (9.6)	0.35 (4.2)	0.44 (5.1)	0.19 (2.3)	0.70	2.10	1.01	2.79	1.32	Y
Average			—	0.39 (4.7)	—	0.23 (2.8)	—	2.36	1.26	—	—	—
Standard deviation			—	0.05 (0.6)	—	0.03 (0.4)	—	0.31	0.17	—	—	—
B_3'	6.4 (4.7)	659 (148)	0.71 (8.6)	0.39 (4.7)	0.49 (6.0)	0.27 (3.2)	1.05	2.32	1.52	3.05	1.50	Y
B_4'	5.0 (3.7)	638 (144)	0.69 (8.3)	0.38 (4.5)	0.48 (5.8)	0.26 (3.1)	1.02	2.25	1.47	2.38	1.45	N
B_3	5.5 (4.1)	744 (167)	0.82 (9.9)	0.52 (6.3)	0.48 (5.5)	0.29 (3.5)	0.77	3.13	1.66	3.06	1.56	N
B_4	5.1 (3.8)	701 (158)	0.88 (10.6)	0.48 (5.8)	0.49 (5.7)	0.26 (3.1)	0.78	2.88	1.46	2.68	1.46	N
B_5	10.5 (7.7)	791 (178)	0.88 (10.5)	0.42 (5.0)	0.51 (5.8)	0.23 (2.8)	0.82	2.49	1.30	5.83	1.66	N
B_6	14.8 (11)	791 (178)	1.00 (11.9)	0.42 (5.1)	0.56 (6.5)	0.23 (2.7)	0.88	2.52	1.27	7.79	1.65	N
Average			—	0.43 (5.2)	—	0.26 (3.1)	—	2.60	1.45	—	—	—
Standard deviation			—	0.06 (0.7)	—	0.02 (0.3)	—	0.34	0.14	—	—	—
C_3'	5.8 (4.3)	612 (138)	0.66 (8.0)	0.29 (3.4)	0.46 (5.5)	0.20 (2.4)	0.98	1.72	1.16	2.76	1.39	Y
C_4'	7.3 (5.4)	673 (151)	0.73 (8.8)	0.32 (3.8)	0.51 (6.1)	0.22 (2.6)	1.08	1.89	1.28	3.48	1.53	N
C_3	5.8 (4.3)	775 (174)	0.86 (10.3)	0.44 (5.3)	0.50 (5.7)	0.25 (3.0)	0.80	2.65	1.46	3.22	1.63	N
C_4	7.6 (5.6)	781 (176)	0.99 (11.8)	0.43 (5.1)	0.55 (6.4)	0.23 (2.8)	0.87	2.55	1.34	4.00	1.63	N
C_5	9.9 (7.3)	858 (193)	0.95 (11.4)	0.35 (4.2)	0.55 (6.3)	0.20 (2.4)	0.89	2.12	1.13	5.50	1.80	Y
C_6	16.5 (12)	872 (196)	1.10 (13.2)	0.36 (4.3)	0.61 (7.1)	0.19 (2.3)	0.97	2.15	1.11	8.68	1.82	N
Average			—	0.36 (4.4)	—	0.21 (2.6)	—	2.18	1.24	—	—	—
Standard deviation			—	0.06 (0.7)	—	0.02 (0.3)	—	0.37	0.14	—	—	—
D_3'	3.1 (2.3)	550 (124)	0.60 (7.2)	0.26 (3.1)	0.41 (5.0)	0.18 (2.1)	0.88	1.54	1.04	1.48	1.25	Y
D_4'	5.5 (4.1)	605 (136)	0.66 (7.9)	0.28 (3.4)	0.45 (5.5)	0.20 (2.4)	0.97	1.70	1.15	2.62	1.38	Y
D_3	4.1 (3.0)	616 (139)	0.68 (8.2)	0.35 (4.2)	0.40 (4.5)	0.20 (2.3)	0.64	2.11	1.16	2.28	1.29	Y
D_4	4.1 (3.0)	634 (143)	0.80 (9.6)	0.35 (4.2)	0.45 (5.2)	0.19 (2.2)	0.70	2.07	1.09	2.16	1.32	Y
D_5	4.4 (3.2)	617 (139)	0.68 (8.2)	0.25 (3.1)	0.40 (4.6)	0.14 (1.7)	0.64	1.52	0.81	2.44	1.30	Y
D_6	5.9 (4.4)	639 (144)	0.81 (9.7)	0.26 (3.2)	0.45 (5.2)	0.14 (1.7)	0.71	1.58	0.81	3.11	1.33	Y
Average			—	0.29 (3.5)	—	0.17 (2.1)	—	1.75	1.01	—	—	—
Standard deviation			—	0.04 (0.5)	—	0.03 (0.3)	—	0.27	0.16	—	—	—

strength prior to failure only in the first three reinforced perimeters and a complete loss in shear strength in the innermost perimeter.

The slab specimens with CFRP laminate Patterns A and D were prone to premature shear failures inside the shear-reinforced zone. Pattern A mostly failed between the second and third shear-reinforcing perimeters. Pattern D always failed between the loading plate face and the first perimeter of shear reinforcement. It is probable that the shear stresses at the corners of the loading plate are considerably higher than those at the face of the loading plate. This can be attributed to the flexural curvature of the slab specimen conforming to the rectangular loading plate. The corners of the loading plate were observed to pierce the slab surface during testing and it is likely that the concrete at these locations fractured in shear initially. The lack of shear reinforcement in the vicinity of the loading plate corners of Pattern A may have allowed these fractures to propagate. Upon reaching the shear reinforcement, the shear cracks have developed considerably and could no longer be contained by the shear reinforcement, permitting them to pass between the shear reinforcing elements. This is reflected by the sudden loss in v_c values within the shear reinforced zone prior to failure. The gradual dissolution of v_c values in the first shear reinforcing perimeter and the lack of apexes in the v_c values in the outer shear reinforcing perimeters for slab Specimen D_6 imply that the shearing forces were not being adequately transmitted to the outer perimeters of shear reinforcement, resulting in the first perimeter being over-stressed and failure of the specimen.

The slab specimens with CFRP Patterns B and C were less likely to fail prematurely within the shear reinforced zone. The lack of sudden strength loss and the presence of apexes in the v_c values for most of the reinforced perimeters imply that the patterns offered sufficient resistance and confinement to prevent the development of large shear cracks and effectively distributed shearing forces to the uncracked concrete outside the shear reinforced zone.

Evaluation of theoretical predictions

Table 2 contains the test results and ultimate load analysis including those using the provisions of the CSA and ACI standards.[4,5] The experimental ultimate loads P_{TEST} have been normalized with respect to $b_o d\sqrt{f_c'}$ and $bd\sqrt{f_c'}$ to make direct evaluation of Eq. (5) and (11). This corresponds to the shear strength of concrete at a distance $d/2$ from the loading plate periphery and from the outermost perimeter of shear reinforcement, respectively. As stated previously, excessive amounts of shear reinforcement were provided to avoid failure of the reinforcement. Table 2 shows that the CSA and ACI standards[4,5] highly underestimated the punching shear capacity of the specimens, in particular those specimens reinforced in shear (refer to P_{TEST}/P_V). This is attributed to the conservative prediction of concrete shear strength. The standards did foresee the occurrence of most shear failures inside the shear-reinforced zone.

The standards specify that the nominal shear stress resistance of concrete be taken as $0.33\sqrt{f_c'}$ (MPa) ($4\sqrt{f_c'}$ (psi)) and $0.167\sqrt{f_c'}$ (MPa) ($2\sqrt{f_c'}$ (psi)) at a distance $d/2$ from the column periphery and from the outermost perimeter of shear reinforcement, respectively. The standards also impose a limit of $0.67\sqrt{f_c'}$ (MPa) ($8\sqrt{f_c'}$ (psi)) on the cumulative shear stress resistance of concrete and the shear reinforcement at a critical section $d/2$ from the column periphery. The v_c values of all of the control specimens and the shear reinforced specimens outside the shear reinforced zone were much greater than $0.33\sqrt{f_c'}$ (MPa) ($4\sqrt{f_c'}$ (psi)) and $0.167\sqrt{f_c'}$ (MPa) ($2\sqrt{f_c'}$ (psi)), respectively, (see $P_{TEST}/bd\sqrt{f'_c}$). Most of the shear reinforced slab specimens attained shear strengths greater than $0.67\sqrt{f_c'}$ (MPa) ($8\sqrt{f_c'}$ (psi)) at a distance $d/2$ from the loading plate periphery (refer to $P_{TEST}/(b_o d\sqrt{f_c'})$).

All the slab specimens with CFRP laminate Pattern D and slab Specimens A_3, A_4, A_6, B_3', C_3', and C_5 did not fail in shear outside the shear reinforced zone. As discussed in Failure characteristics, high shear stresses initiate failure at the corners of the loading plate. This is confirmed by the findings of Sherif and Dilger.[10] Shear reinforcing Pattern A did not have shear reinforcing at the loading plate corners as recommended by the ACI standards[5] and was incapable of confining the shear fractures initiating from them. Pattern D had shear reinforcement at the corners but was incapable of transferring shear stresses sufficiently away from the loading plate. Slab Specimens B_3' and C_3' had consecutive shear reinforcing perimeters spaced at $0.75d$. Equation (7) specifies that for this spacing the shear stress shall not exceed $0.5\sqrt{f_c'}$ (MPa) ($6\sqrt{f_c'}$ (psi)) at a critical section perimeter $d/2$ from the column periphery. Both these specimens exceeded this limitation (refer to $P_{TEST}/(b_o d\sqrt{f_c'})$).

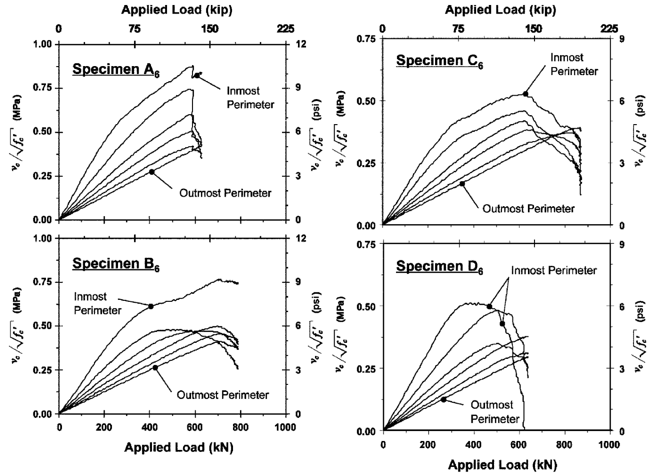

Fig. 15—Concrete shear strength for critical sections in-line with shear reinforcement.

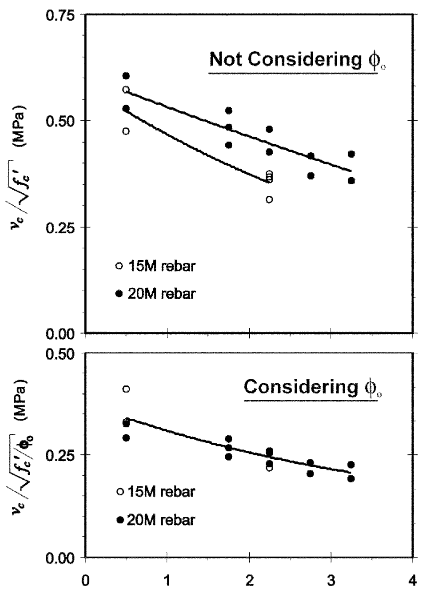

Fig. 16—Shear strength of concrete outside shear-reinforced zone.

Design consideration

The conservative shear strength of concrete specified in the CSA A23.3-04 and ACI 318-05 standards can be attributed to the assumption that the shear to flexural capacity ratio is almost unity. Shear strength is known to decrease as the extent of flexural yielding in the slab increases. The decrease in shear strength is attributed to the loss in membrane action as a consequence of greater flexural yielding.[11] Hognestad[12] identified the influence of flexural yielding and introduced the variable ϕ_o equal to the ratio of shear to flexural capacity. A properly designed slab has a flexural strength less than the shear strength. To simplify design procedures, the ACI and CSA standards[4,5] assume ϕ_o equal to unity, which is conservative because a value less than unity has higher nominal shear stress resistance, as is evident in the test results presented herein.

Using the ultimate capacity and the specified[4,5] critical section area, Fig. 16 plots the nominal shear resistance of concrete for the slab specimens with shear failures outside the shear-reinforced zone (Table 2), with and without

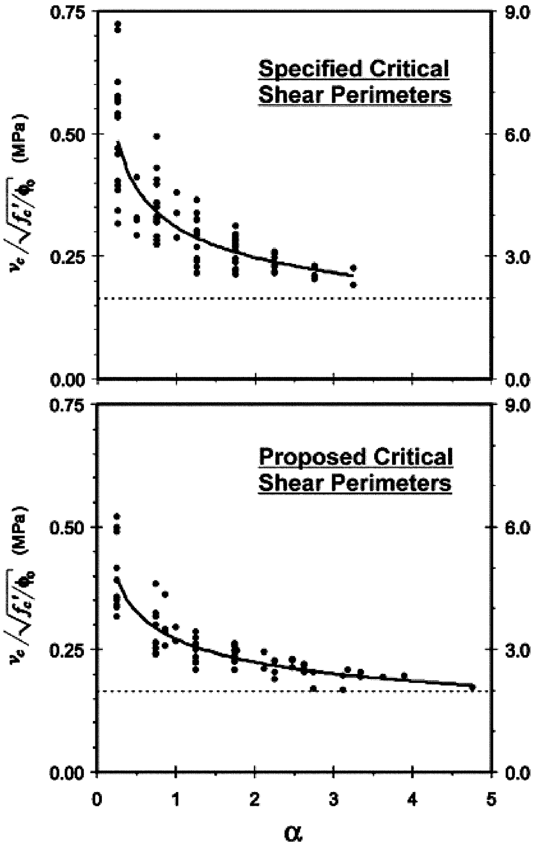

Fig. 17—Shear strength of concrete within shear reinforced zone.

consideration of the flexural to shear capacity ratio. The capacities have been normalized with respect to concrete strength. The shear-to-flexural capacity ratio ϕ_o is taken as that for the respective control specimen of each slab (Table 1). The shear strength is referenced with respect to α, the ratio of distance between the loading plate periphery and the critical shear section to the effective slab thickness. Evident in Fig. 16 is that the shear strength of concrete is lower in specimens that have larger ϕ_o values (those slab specimens with 15 M flexural reinforcement bars) and that the CSA and ACI standards[4,5] specified concrete shear strengths of $0.33\sqrt{f_c'}$ (MPa) ($4\sqrt{f_c'}$ (psi)) and $0.167\sqrt{f_c'}$ (MPa) ($2\sqrt{f_c'}$ (psi)) for the control and shear-reinforced specimens, respectively, are conservative. Also evident is that this disparity in shear strength when compared with the CSA and ACI provisions appears to be mitigated when concrete strength is normalized with respect to ϕ_o. The shear strength of concrete is approximately $0.33\sqrt{f_c'}$ (MPa)/ϕ_o ($4\sqrt{f_c'}$ (psi)/ϕ_o) at a distance α = 0.5 and diminishes asymptotically toward $0.167\sqrt{f_c'}$ (MPa)/ϕ_o ($2\sqrt{f_c'}$ (psi)/ϕ_o) at a distance $\alpha > 3$ (refer also to $P_{TEST}/bd\sqrt{f_c'/\phi_o}$ in Table 2). The cumulative nominal shear stress resistance at a distance $d/2$ from the loading plate periphery does not exceed $0.67\sqrt{f_c'}$ (MPa)/ϕ_o ($8\sqrt{f_c'}$ (psi)/ϕ_o) for any of the specimens (refer to $P_{TEST}/b_od\sqrt{f_c'/\phi_o}$ in Table 2).

From the observed shear fractures (Fig. 10), it can be concluded that the influence of the rectangular loading plate to impart a rectangular shear stress distribution dissipates with distance from the loading plate and that the failure planes furthest away from the loading plate are of circular shape. The lower portion of Fig. 4 depicts the proposed critical shear perimeters that are circular at the corners. In this way, the proposed perimeters are near rectangular immediately adjacent to the loading plate and become near circular furthest away from the loading plate. Using both the specified and the proposed critical perimeters, concrete strength is determined by Eq. (14) through (16) for each peripheral line of shear reinforcement for all specimens except those of Pattern D (Fig. 17). Pattern D was not included due to its failure to effectively distribute shear stresses among the shear reinforcement. The fact that the interior perimeters of shear reinforcement Pattern C are no longer in line with the proposed peripheral lines (Fig. 4), only the outermost perimeter is plotted. It is clear that the scatter in the results using the specified critical shear perimeters is considerably reduced with the use of the proposed critical shear perimeters and that the results of Fig. 16 that include ϕ_o are further substantiated.

In Table 2, column P_{TEST}/P_V' has revised code predictions based on the proposed critical shear sections defined in Fig. 4 and concrete strengths normalized with respect to ϕ_o. It is apparent that these predictions are much closer to actual but still conservative. Because the CSA and ACI standards specify concrete shear strength of $0.167\sqrt{f_c'}$ (MPa) ($2\sqrt{f_c'}$ (psi)) irrespective of how far the shear reinforcement is extended, the capacity will be underestimated in cases where the shear reinforcement is appropriately distributed and extends to a distance $\alpha < 5$. Sherif and Dilger[10] experienced shear strength less than $0.2\sqrt{f_c'}$ (MPa) ($2.4\sqrt{f_c'}$ (psi)) at $\alpha > 5$ and recommend that shear reinforcement not be extended beyond $\alpha = 4.5$. The shear reinforcement was not extended sufficiently in this investigation to evaluate this parameter.

CONCLUDING REMARKS

An innovative technique to retrofit concrete slabs for enhancing their punching shear capacity was first suggested by the authors in 2000.[2] Further tests were completed and reported in 2002.[3] This extensive experimental work is summarized in this paper. The approach involves reinforcing the slab in the vicinity of a column with FRP laminates through an elaborate pattern of vertical holes. Conceptually, the slab is stitched with FRP fabric and the holes are filled with epoxy. The experimental program consisted of 32 1.5 m (4.9 ft) square and 150 mm (5.9 in.) deep slabs under concentric load to validate the proposed technique. Results from four specimens of the pilot series are not included herein because anchorage of FRP laminates resulted in increased flexural strength of the slabs in addition to the enhanced shear capacity. Results from 28 specimens are presented herein based on which the following conclusions can be drawn:

1. The slab specimens retrofitted with CFRP laminate shear reinforcement demonstrated a substantial increase in shear strength, ductility, and energy dissipation capacity. Shear strength increase of over 80% and enhancement of ductility of over 700% were observed;

2. Greater increases in ductility, capacity, and audible distress are exhibited with greater numbers of shear reinforcing perimeters, particularly in shear-reinforcing patterns with closer spacing of shear reinforcement along peripheral lines;

3. Within a group of slab specimens with equal potential shear critical sections outside the shear-reinforced zone, larger consecutive spacing of shear reinforcement did not have any adverse effect on strength or ductility but caused greater degrees of concrete cracking and increased the probability of shear failures within the shear-reinforced zone;

4. Closer spacing of shear reinforcement resulted in greater improvements in the behavior of slabs. Thus, shear-reinforcing Patterns A and D (Fig. 4) exhibited comparatively lower improvements in ductility and shear capacity. The patterns were susceptible to premature shear failures within the shear-reinforced zone. Patterns B and C exhibited comparatively higher ductility and shear capacity improvements. These patterns offered effective confinement to prevent the development of shear failure within the shear-reinforced zone;

5. The proposed critical shear section perimeters with rounded corners in the manner depicted in Fig. 4 best represent the behaviors of the shear reinforcement patterns tested in this research program; and

6. The nominal shear stress resistance of concrete varies with distance from the loading area and can be taken as $0.33\sqrt{f'_c}$ (MPa)/ϕ_o ($4\sqrt{f'_c}$ (psi)/ϕ_o) at $\alpha = 0.5$, decreasing asymptotically toward $0.167\sqrt{f'_c}$ (MPa)/ϕ_o ($2\sqrt{f'_c}$ (psi)/ϕ_o) at $\alpha > 4$, where ϕ_o is the shear to flexural capacity ratio and α is the ratio of the distance between the loading area periphery and the critical shear perimeter to the effective slab thickness. All the slab specimens had cumulative shear strength less than $0.67\sqrt{f'_c}$ (MPa)/ϕ_o ($8\sqrt{f'_c}$ (psi)/ϕ_o) at $\alpha = 0.5$.

ACKNOWLEDGMENTS

The research reported herein was funded by grants from the Natural Sciences and Engineering Council of Canada (NSERC) and ISIS Canada, an NSERC Network of Centres of Excellence. Technical and financial support from R. J. Watson Inc. of East Amherst, N. Y., Fyfe Co. LLC of San Diego, Calif., and Premier Corrosion Protection Services Inc. of Oakville, Ontario, Canada, is gratefully acknowledged. The experimental work was carried out at the Structures Laboratories of the University of Toronto, Toronto, Ontario, Canada. Thanks are extended to O. Bayrak for his help in the experimental program during his post-doctoral tenure at the University of Toronto.

NOTATION

A_{CFRP} = width of CFRP shear laminate on concentric line parallel to loading area periphery
b = shear critical section perimeter d/2 from outermost peripheral line of shear reinforcement
b_o = perimeter of shear critical section d/2 from loading area periphery
c = rectangular loading plate width
d = effective slab thickness for shear
F_{CFRP} = total tensile force in peripheral line of CFRP laminates
f'_c = concrete cylinder compressive strength
f_U = ultimate strength of flexural reinforcement
f_Y = yield strength of flexural reinforcement
L = width of simply supported slab
m_r = flexural capacity of slab per unit width
P = instantaneous applied load
P_{cont} = applied ultimate load during testing of respective control specimen
P_{Test} = applied ultimate load during testing
P_V = CSA A23.3-04 and ACI 318-05 standards punching shear capacity
P'_V = P_V values based on f'_c normalized with respect to ϕ_o and critical shear perimeters defined in Fig. 4(b)
P_Y = yield line theory flexural capacity
s = spacing between consecutive peripheral lines of shear reinforcement parallel to loading area periphery
s_o = distance between loading area periphery and first peripheral line of shear reinforcement
U_{80} = strain energy absorbed up to 80% of ultimate load, beyond the peak
$(U_{80})_{cont}$ = strain energy absorbed up to 80% of ultimate load, beyond peak of respective control specimen
V_f = shear force due to factored loads
v_{CFRP} = nominal shear stress resistance of CFRP laminate shear reinforcement
v_c = nominal shear stress resistance of concrete
v_f = nominal shear stress due to factored loads
v_r = nominal shear stress resistance
α = ratio of distance between loading area periphery and critical shear section to effective shear slab thickness
α_s = support type modification factor
β_c = ratio of long to short side of loading area periphery
ϕ_c = resistance factor for concrete
ϕ_o = calculated ratio of shear to flexural capacity, P_V/P_Y
θ = angle of inclination of principle compressive stresses from slab surface
ρ = percent flexural reinforcement

REFERENCES

1. Sheikh, S. A., and Homam, S. M., "A Decade of Performance of FRP-Repaired Concrete Structures," *Proceedings of the Second International Workshop on Structural Health Monitoring of Innovative Civil Engineering Structures*, Winnipeg, Manitoba, Canada, Sept. 2004, pp. 525-534.

2. Sissakis, K., and Sheikh, S. A., "The Use of CFRP Strands to Improve the Punching Shear Resistance of Concrete Slabs," *Research Report*, Department of Civil Engineering, University of Toronto, Toronto, Ontario, Canada, 2000, 86 pp.

3. Sissakis, K., "Strengthening of Concrete Slabs for Punching Shear with CFRP Laminates," MASc thesis, Department of Civil Engineering, University of Toronto, Toronto, Ontario, Canada, 2002, 215 pp.

4. CSA-A23.3-04, "Design of Concrete Structures," Canadian Standards Association, Rexdale, Ontario, Canada, 2004, 214 pp.

5. ACI Committee 318, "Building Code Requirements for Structural Concrete (ACI 318-05) and Commentary (318R-05)," American Concrete Institute, Farmington Hills, Mich., 2005, 430 pp.

6. Criswell, M. E., and Hawkins, N. W., "Shear Strength of Slabs: Basic Principle and their Relation to Current Methods of Analysis," *Shear in Reinforced Concrete*, SP-42, V. 2, 1974, pp. 641-678.

7. CPCA, *Concrete Design Handbook,* Canadian Portland Cement Association, Ottawa, Ontario, Canada, 1995.

8. Joint ACI-ASCE Committee 421, "Shear Reinforcement for Slabs (ACI 421.1R-99)," American Concrete Institute, Farmington Hills, Mich., 1999, 15 pp.

9. Johansen, K. W., *Yield Line Theory*, Cement and Concrete Association, London, 1962, 181 pp.

10. Sherif, A. G., and Dilger, W. H., "Critical Review of the CSA A23.3-94 Punching Shear Provisions for Interior Columns," *Canadian Journal of Civil Engineering*, V. 23, 1996, pp. 998-1011.

11. Hawkins, N. M., and Mitchell, D., "Progressive Collapse of Flat Plate Structures," ACI JOURNAL, *Proceedings* V. 76, No. 7, July 1979, pp. 775-808.

12. Hognestad, E., "Shear Strength of Reinforced Concrete Column Footings," ACI JOURNAL, *Proceedings* V. 50, No. 11, Nov. 1953, pp. 189-208.